Ordering in Supramolecular Elastomer−Amphiphile Systems. 4. Vinylpyridine−Divinylbenzene Networks with Alkylphenols

M. C. Luyten, G. O. R. Alberda van Ekenstein, J. Wildeman, and G. ten Brinke*

Department of Polymer Science and Materials Science Center, University of Groningen, Nijenborgh 4, 9747 AG Groningen, The Netherlands

J. Ruokolainen and O. Ikkala*

Department of Engineering Physics and Mathematics, Helsinki University of Technology, P.O. Box 2200, FIN-02015 HUT, Espoo, Finland

M. Torkkeli and R. Serimaa

Department of Physics, University of Helsinki, P.O. Box 9, FIN-00014, Helsinki, Finland

Received June 4, 1998; Revised Manuscript Received September 28, 1998

ABSTRACT: We report here on the extension to elastomers of the idea of inducing nanoscale ordering in supramolecular polymer systems based on the principle of hydrogen bonding between amphiphiles and (block co-)polymers. Three different networks have been synthesized using 4-vinylpyridine and divinylbenzene (0.5, 1.0, and 2.0 mol %, respectively) and are further complexed with pentadecylphenol or nonadecylphenol. For low degrees of cross-linking (0.5 and 1.0 mol % divinylbenzene), mesomorphic structures are formed, and order−disorder transitions are observed by small-angle X-ray scattering (SAXS) and differential scanning calorimetry. For the highest degree of cross-linking (2.0 mol % divinylbenzene), mesomorphic structures is no longer observed. The presence of ordered lamellar structures is confirmed by transmission electron microscopy (TEM). SAXS and TEM clearly reveal the deteriorating effect of an increasing degree of cross-linking on the structure formation.

Introduction

Polymer−amphiphile systems have been studied extensively in recent years, and it is now well established that these systems can give rise to well-ordered mesoscopic structures. Amphiphiles that contain mesogenic groups have been bonded to homopolymers by ionic interactions,[1−4] molecular recognition,[5] and coordination bonding[6] leading to liquid crystalline complexes. Likewise, flexible nonmesogenic amphiphiles can be complexed with homopolymers using ionic interactions[7−11] and hydrogen bonding[12−15] in which case the associated molecular structures are essentially supramolecular comb copolymers, resulting from the complexation between linear polymers and amphiphiles. They offer unique opportunities to study systematically the influence of the composition, determined by the amount and length of the amphiphilic molecules, on the morphology and the phase behavior. In this work nonmesogenic amphiphiles are considered.

The phase behavior of the polymer−amphiphile systems can be manipulated in a rather straightforward way by controlling the amphiphile head−polymer attraction and the amphiphile tail−polymer repulsion. The most simple systems studied consisted of poly(4-vinylpyridine) (P4VP) complexed with different types of amphiphiles. Our efforts concentrated on hydrogen-bonded amphiphiles of which the alkylphenols, notably pentadecylphenol (PDP) and nonadecylphenol (NDP), offer a highly interesting balance between attraction and repulsion. In many cases order−disorder transitions from a high-temperature isotropic state to a microphase separated lamellar morphology were observed. Besides small-angle X-ray scattering (SAXS), we were able to image lamellar structures with transmission electron microscopy (TEM) in the case of the longest surfactant NDP.[16] When the complexation is combined with block copolymers of polystyrene (PS) and P4VP, structures inside structures are formed.[17] In the case of complexation with NDP, i.e., PS-*block*-P4VP(NDP)$_{1.0}$ (subscript denotes number of phenol groups per pyridine group), we were able to image the layered structures inside the P4VP containing domains of the microphase separated block copolymer system.[17]

A related class of polymer systems consists of polymer networks with pendant side chains that offer possibilities to combine nanoscale structure formation and elastomeric properties. Especially in the field of side chain liquid crystalline polymers, considerable attention has been given to these kinds of materials.[18−20] The phase behavior of side chain liquid crystalline polymer networks is found to be analogous to the corresponding linear polymers. However, the materials show additional interesting behavior due to the coupling between liquid crystalline and network properties which leads to perfectly oriented liquid crystalline domains under relatively small strains. So far, investigations dealing with polymer network−amphiphile systems concerned mainly polyelectrolytes with oppositely charged surfactants and addressed the structures formed in a gel, i.e., a system consisting of a polymer network, surfactant molecules, and additional solvent.[21−23]

Here we will report on a study of nanoscale ordering in "dry" polymer network−amphiphile systems with complexation obtained by hydrogen bonding. As in the case of liquid crystalline elastomers, we ultimately hope to profit from the mechanical orientability. But first we will have to show that the principles developed for the

* Corresponding authors.

10.1021/ma9808833 CCC: $15.00
Published on Web 12/03/1998

linear case also work here. As a model system we took networks obtained by copolymerization of 4-vinylpyridine and divinylbenzene, which allows for a direct comparison with our results on the linear polymer systems. Furthermore, pentadecylphenol and nonadecylphenol were again used as the hydrogen-bonding amphiphile. The properties and the phase behavior will be discussed as a function of cross-link density and amphiphile concentration as determined by differential scanning calorimetry, small-angle X-ray scattering, and transmission electron microscopy.

Experimental Section

Materials. 3-Pentadecylphenol (PDP) was purchased from Aldrich and was first dried in a vacuum oven at 40 °C for several days. The linear poly(4-vinylpyridine) (P4VP) was purchased from Polyscience Europe GmbH. The viscosity averaged molar mass was $M_v = 49\,000$ g/mol. The synthesis and characterization of 4-nonadecylphenol (NDP) are described in ref 20.

The cross-linked polymer system was synthesized. 4-Vinylpyridine (4VP) was provided by Merck-Schuchardt and purified by distillation to remove inhibitor. Dimethylformamide (DMF) was distilled before use. The initiator AIBN was recrystallized from methanol before use. *p*-Divinylbenzene (DVB) was isolated from a commercial mixture of isomers[24] by adapting the literature procedure using bromination and debromination.[25] 4VP and 0.5, 1, or 2 mol % DVB were dissolved in DMF; 0.5 mol % AIBN was added. The polymerization took place for 40 h at 65 °C under nitrogen. The network gel was washed with tetrahydrofuran (THF) in a Soxhlet for 3 days to remove the DMF and dried in a vacuum oven for several days at 40 °C.

P4VPy(PDP)$_x$ (y denotes mol ‰ DVB, x denotes number of phenol groups per pyridine group) complexes were made from chloroform ($CHCl_3$) solutions. Samples were prepared with x varying from $x = 0.15$ to $x = 2.0$ and for $y = 0$, 5, 10, and 20. PDP was dissolved in $CHCl_3$, and subsequently P4VPy was added. The mixture was stirred for 5 days at room temperature. Then the $CHCl_3$ was evaporated at 80 °C. The samples were subsequently dried in a vacuum oven at 40 °C for a week.

Infrared Spectroscopy. The Fourier transform infrared (FTIR) measurements were performed on a Mattson Galaxy 6021 FTIR spectrophotometer in combination with a MCT detector. The linear polymer sample P4VP was dissolved in $CHCl_3$ and cast onto a potassium bromide (KBr) window. The network polymer samples P4VPy(PDP)$_x$ were powdered together with KBr and pressed to pellets.

Differential Scanning Calorimetry (DSC). A Perkin-Elmer DSC-7 was used to investigate the samples. The pure polymer network sample was annealed for 5 min at 200 °C, then quenched to 50 °C, kept for 5 min at this temperature, and subsequently heated with 10 °C/min to 200 °C. The P4VPy(PDP)$_x$ samples were annealed at 200 °C for 5 min and then cooled at 10 °C/min to −50 °C. They were kept at this temperature for 5 min and subsequently heated at a heating rate of 10 °C/min.

Small-Angle X-ray Scattering (SAXS). Cu Kα radiation ($\lambda = 1.542$ Å) was monochromatized by means of the combined action of a Ni filter and a totally reflecting mirror (Huber small angle chamber 701). The sealed Cu anode fine focus X-ray tube was powered by a Siemens Kristalloflex 710H. The scattered radiation was detected in the horizontal (beam width) direction by a linear one-dimensional position sensitive proportional counter (MBraun OED-50M). A narrow slit was used before the sample to minimize the background scattering. The primary beam is narrow (full width at half-maximum (fwhm) < 0.002 Å^{-1}) compared to its length (fwhm $= 0.027$ Å^{-1}) at the sample. Together with the detector height profile, the fwhm of the instrumental function was 0.048 Å^{-1}. The smallest achievable k is only ca. 0.02 Å^{-1} by using the wave vector $k = 4\pi/\lambda \sin\theta$, where 2θ is the scattering angle. The samples are cooled from 100 to 20 °C with intervals of 2 °C. Every frame is 600 s.

Transmission Electron Microscopy. Bulk samples of P4Vy(NDP)$_{1.0}$ ($y = 5$, 10, 20) for TEM characterization were imbedded in epoxy and cured at 60 °C overnight. Ultrathin sections (30−50 nm) were cut from the embedded specimen using a Reichert Ultracut E ultramicrotome and a diamond knife at room temperature. Sections were picked up on 600 mesh copper grids, and to enhance contrast, the microtomed sections were stained in the vapor of I_2 crystals. Bright field TEM was performed on a JEOL-1200EX transmission electron microscope with tungsten filament operating at an accelerating voltage of 60 kV.

Results and Discussion

Homopolymer P4VP complexed with PDP has been extensively investigated. For nominally full complexation, i.e., P4VP(PDP)$_{1.0}$, an order−disorder transition (ODT) occurs at around 60 °C from a homogeneous state to a microphase separated state in which the nonpolar tail of the hydrogen-bonded PDP microphase separates from the P4VP polymer to form a lamellar structure with a long period of the order of 35 Å.[14,15] To explore the corresponding concepts for elastomeric materials, polymer networks were polymerized by a copolymerization of 4-vinylpyridine (4VP) and divinylbenzene (DVB). The networks will be denoted as P4VPy, where y denotes the mole ‰ of divinylbenzene in the 4VP/DVB mixture. Three different networks were synthesized: P4VP5, P4VP10, and P4VP20. Assuming that all DVB is reacted completely, for which we will present evidence further on, we have approximately 1000/y units of 4VP for every DVB unit. Consequently, the average chain length between cross-links, N_y, satisfies $N_y = 500/y$, expressed in the number of monomer units. Hence, the cross-link density Y is given by

$$Y = \frac{1}{N_y} = \frac{y}{500} \tag{1}$$

The different networks correspond to a chain length between entanglements given by $N_y = 100$, 50, and 25, respectively. Since the length of the PDP molecule is comparable to $N_y = 10$, this indicates that the relatively small mesh size of the most densily cross-linked network might severely interfere with the tendency to form microphase separated structures.

Polymer Network Characterization. To analyze the presence of DVB in P4VPy and to find out whether any unsaturated double bonds due to unreacted DVB are left in the sample, FT-IR spectra of DVB, P4VP, and P4VPy were compared. The spectra of cross-linked P4VPy show an extra peak at 1510 cm^{-1} not present in pure P4VP. This peak is due to the aromatic stretching in the benzene ring, which can be attributed to the presence of divinylbenzene, and confirms that DVB is actually incorporated in the P4VPy polymer network. No signs of the characteristic C−H deformation vibration of the vinyl group CH═CH$_2$ at 905 cm^{-1} are found in P4VPy, which would have been present in the case of incompletely reacted DVB. It confirms that, within experimental error, the reaction of 4-VP with DVB has been complete and that the nominal amount of DVB added to the reaction equals the actual number of cross-links. This is also stated in the literature[26] and will now be corroborated further by an analysis of the glass transition behavior.

DSC measurements were performed to determine the glass transition temperature T_g of the cross-linked polymer P4VPy. The results are shown in Figure 1

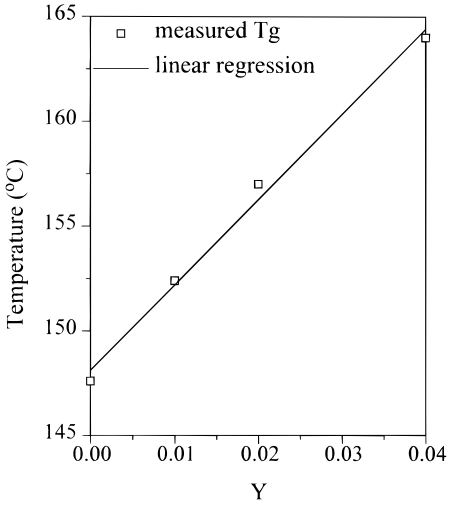

Figure 1. Glass transition temperatures as a function of cross-link density *Y*. Solid line represents a fit with the DiMarzio equation (eq 2) for $K = 0.97$.

together with the T_g of the homopolymer P4VP. A linear relation between the cross-link density and T_g is found, which, as previous studies showed, is exactly as should be expected for a low degree of cross-linking. DiMarzio[27] derived a relation between the cross-link density *Y* and T_g given by

$$\frac{T_g(Y) - T_g(0)}{T_g(0)} = \frac{KY}{1 - KY} \qquad (2)$$

Here $T_g(Y)$ is the T_g at cross-link density *Y*, $T_g(0)$ is the T_g for non-cross-linked polymer, and *K* is a pure number whose value is to first order independent of material. Indeed, for small *Y* the denominator of the right-hand side of eq 2 is about 1, and the T_g is linearly dependent on the cross-linking density *Y*. A fit of our data to eq 2 gives a value of $K = 0.9671$, which seems very reasonable compared to a value of $K = 0.9033$ determined for polystyrene cross-linked with DVB.[28] This supports the assertion based on the FTIR data that to a good approximation all the DVB has reacted to form cross-links.

Polymer Network-Surfactant Complex. FT-IR. Infrared measurements were performed to study the association between P4VP*y* and PDP. Previous studies on linear P4VP(PDP)$_x$ showed that the most affected bands are those concerned with the stretching modes of the pyridine ring: 1597, 993, and 627 cm^{-1} for P4VP. Also, the band at 1415 cm^{-1} should shift on formation of a hydrogen bond. These effects are a consequence of changes in the electronic distributions in the pyridine ring. FT-IR spectra of P4VP*y*(PDP)$_x$ were measured for $y = 5$, 10, and 20 and various values of *x*. The most affected bands are given in Figure 2 for the system P4VP5(PDP)$_x$ together with the spectra of pure P4VP5 and pure PDP. The other polymer networks show a similar behavior. Figure 2 shows that the bands at 1597 and 993 cm^{-1} shift to 1603 and 1001 cm^{-1} upon formation of a hydrogen bond. Note, however, that it is very difficult to determine the actual degree of complexation based on these bands, due to the nearby absorption peaks of pure PDP and DVB. The shift of the 1415 cm^{-1} band to 1423 cm^{-1} on the other hand can be observed very clearly because there is no overlapping absorption of pure PDP. On the basis of this band, we

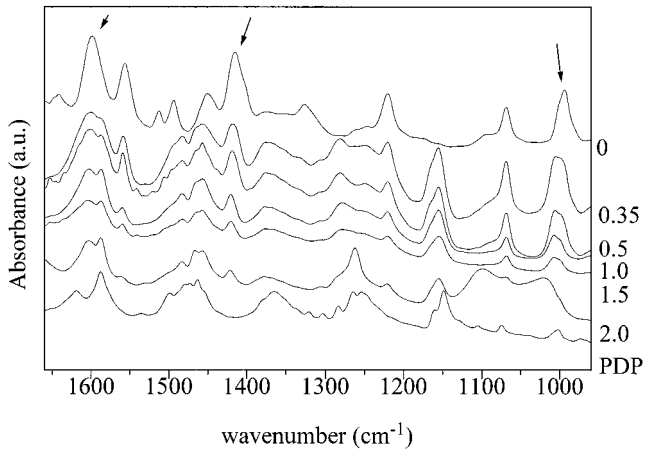

Figure 2. FT-IR spectra of P4VP5(PDP)$_x$ for $x = 0.35$, 0.5, 1.0, 1.5, and 2.0, together with pure P4VP5 and PDP.

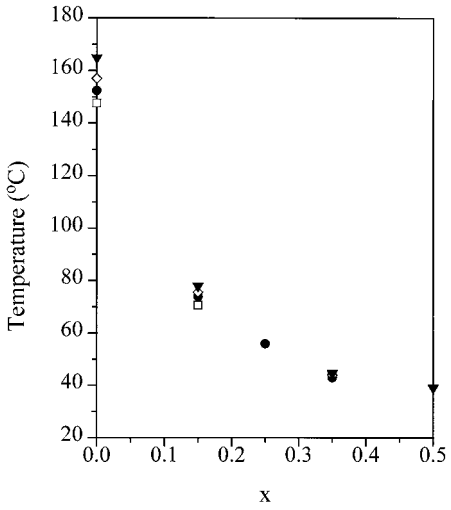

Figure 3. Glass transition temperatures as a function of *x* for P4VP(PDP)$_x$ (□), P4VP5(PDP)$_x$ (●), P4VP10(PDP)$_x$ (◇), and P4VP20(PDP)$_x$ (▼).

can conclude that the association is nearly complete at $x = 1.0$. The same behavior is seen for P4VP(PDP)$_x$, P4VP10(PDP)$_x$, and P4VP20(PDP)$_x$.

Differential Scanning Calorimetry. The glass transition temperatures of P4VP(PDP)$_x$ and P4VP*y*(PDP)$_x$ were measured as a function of the amount *x* of amphiphile. For $y = 20$, a T_g could only be detected for the samples with $x \leq 0.5$, whereas for $y = 5$ and 10 as well as linear P4VP, a T_g was only observed for $x \leq 0.35$. As shown in Figure 3, all glass transition temperatures decrease with increasing amount of PDP in a similar fashion. This behavior is comparable with polymer−solvent systems, where the addition of solvent also plasticizes the polymer. For comb copolymers a reduction in the glass transition temperature as a function of the side chain density was reported by Jordan,[29] who measured the T_g of various copolymers where one of the monomers carried a long side chain. The fact that we do not observe a glass transition for *x* exceeding 0.5 (respectively 0.35) is due to either the crystallization of the alkyl side chains or the order−disorder transition from a homogeneous state to a microphase separated state. We will turn our attention to these issues next.

Order−Disorder Transition. It is now well documented that P4VP (PDP)$_x$ samples undergo an order−disorder transition from a homogeneous state to a microphase separated layered state.[14,15] In the case of

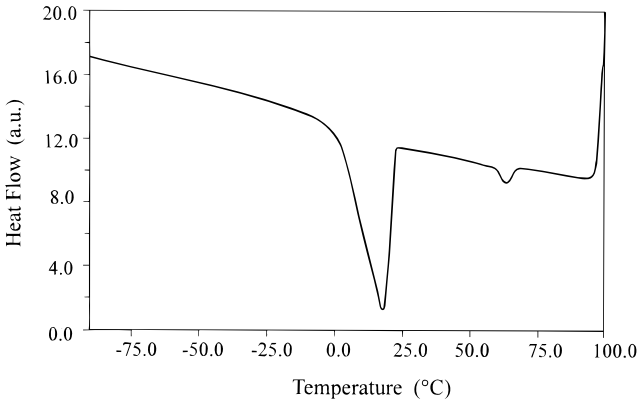

Figure 4. DSC thermogram recorded during cooling at 10 °C/min of P4VP5(PDP)$_{1.0}$. Note ODT peak at 60 °C and crystallization peak at 17 °C.

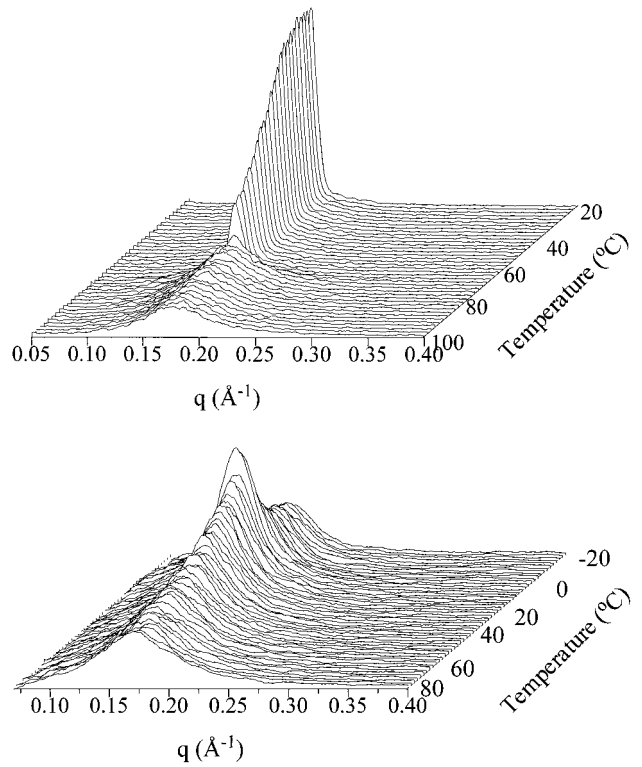

Figure 5. SAXS intensity curves as a function of temperature: (a, top) P4VP5(PDP)$_{1.0}$ and (b, bottom) P4VP20(PDP)$_{0.85}$.

P4VP an ODT was only observed for samples with $x \leq 1.5$. For values of $x > 1$ the transition temperature decreases fast, and for $x > 1.5$ the crystallization temperature of PDP is located above the order−disorder transition temperature. A high degree of cross-linking is expected to strongly interfere with the possibility to form ordered structures, eventually suppressing the ODT all together. A low degree of cross-linking, on the other hand, is not expected to change the phase behavior in an essential way.

In a DSC scan, the ODT shows up as a weak first-order transition. Figure 4 shows a representative thermogram of P4VP5(PDP)$_{1.0}$, obtained by cooling with 10 °C/min, displaying an ODT at 62 °C and a crystallization transition at 12 °C. The ODT is accompanied by an enthalpy of transition of about 2 J/g. Since the glass transition of the homogeneously mixed state would be considerably below 60 °C, it can no longer be observed. The microphase separation leads to alternating P4VP containing layers and alkyl layers, which subsequently crystallize.

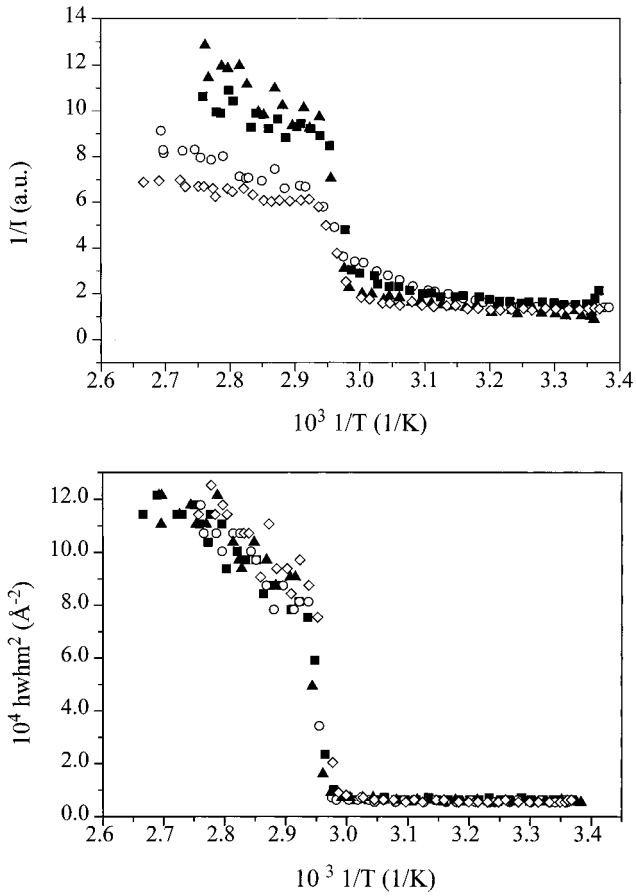

Figure 6. Plots versus inverse temperature $1/T$ of (a, top) inverse intensity at peak maximum $1/I_{max}$ and (b, bottom) square of half-width at half-maximum of scattering peak (hwhm)^2 for P4VP5(PDP)$_x$, $x = 0.5$ (■), 0.85 (○), 1.0 (▲), 1.5 (◇).

Figure 5a presents the SAXS results for P4VP5-(PDP)$_{1.0}$ obtained during cooling from the homogeneous melt at 100 °C to 23 °C at 0.4 °C/min. As usual, a scattering peak at finite wavelength q^* is present at high temperatures due to the correlation hole effect.[30,31] Around 65 °C a strong increase in intensity is observed, signaling the transition from a homogeneous disordered state to an ordered microphase separated lamellar state. In general, the ODT in block copolymer systems can be determined from these data by plotting as a function of the inverse temperature $1/T$ either the inverse intensity at the peak maximum $1/I_{max}$, the characteristic length scale, or the square of the half-width of the half-maximum (hwhm)^2 of the scattering peak.[32−34]

We applied the above methods to all our samples showing an order−disorder transition. The results for the case of P4VP05(PDP)$_x$ ($x = 0.5$, 0.85, 1.0, 1.5) are presented in Figure 6. The scatter in the data for $2\pi/q^*$ (not shown) at temperatures above the order−disorder transition is too large to be useful for an accurate determination of the ODT. Figure 6a presents $1/I_{max}$ versus $1/T$ and shows that a sudden discontinuous drop is found around 65 °C. Surprisingly, the order−disorder temperature thus defined is nearly independent of the amount of PDP. The same conclusion follows from the plots of (hwhm)^2 versus $1/T$ (Figure 6b). Another remarkable observation is that in the latter case all the data collapse together below the order−disorder tem-

Table 1. Long Period and Order−Disorder Transition Temperatures[a]

	$x = 0.5$		$x = 0.85$		$x = 1.0$		$x = 1.5$	
	D (Å)	T_{ODT} (°C)	D (Å)	T_{ODT} (°C)	D (Å)	T_{ODT} (°C)	D (Å)	T_{ODT} (°C)
P4VP(PDP)$_x$	39.5	53	38.5	59	36.5	55	35	38
P4VP5(PDP)$_x$	38.5	59	38.0	62	38.0	63	38.0	61
P4VP10(PDP)$_x$	38.5	58	38.5	62	38.5	62	38.0	40

[a] The order−disorder transition temperatures represent DSC data.

perature. This implies that the average thickness of a stack of alternating polar−nonpolar layers is independent of the amount of PDP in the range investigated. The P4VP10(PDP)$_x$ systems behave in a similar way. Higher degrees of cross-linking obviously must interfere with the possibility of spontaneous self-organization. That this is indeed the case is clearly demonstrated by the P4VP20(PDP)$_x$ samples, which exhibit only broad scattering maxima in the SAXS data corresponding to the usual correlation hole peaks; cf. the example given in Figure 5b for P4VP20(PDP)$_{0.85}$. A clear order−disorder transition is no longer observed, unquestionably because of the network constraints, i.e., the strongly reduced mesh size. However, the SAXS data in Figure 5b do show an increase in scattering intensity, reminiscent of the stronger fluctuations giving rise to the order−disorder transition in less densely cross-linked systems. With DSC only peaks corresponding to crystallization of the PDP molecules were seen.

Table 1 contains the long period of the ordered structures as a function of x at room temperature for the network systems with $y = 5$ and 10 compared with the non-cross-linked system, the latter taken from refs 16 and 35. These data have to be considered with care since the long periods of P4VP(PDP)$_{1.5}$ and P4VP10(PDP)$_{1.5}$ represent the long periods just after the ODT and hence represent weak segregation regime data. All the others already correspond to the strong segregation regime. The values of the ODT for the networks and P4VP(PDP)$_x$ as obtained with DSC are also presented in Table 1. The real equilibrium ODT temperatures will be slightly higher because of the scan speed of 10 °C/min employed. In all cases the order−disorder temperature is slightly higher for the networks than for linear P4VP.

These results demonstrate that the differences between the linear system and the slightly cross-linked systems ($y = 5$, 10) are small. This is also confirmed by Figure 7, which presents a characteristic TEM picture showing the ordered lamellar structure for P4VP5(NDP)$_{1.0}$ (Figure 7B). The picture is very similar to the recently published data[16] on the linear polymer system, i.e., P4VP(NDP)$_{1.0}$ as is also clear from Figure 7A, which presents another example of this system. The TEM study of P4VP20(NDP)$_{1.0}$ shows only a very faint remnant ordering (Figure 7C). Although the pictures are for the slightly longer NDP amphiphile, they are in excellent agreement with the SAXS and DSC data for the corresponding PDP systems.

Chu et al.[22,23] studied gels of poly(diallyldimethylammonium chloride) and sodium dodecyl sulfate and found that the SAXS profiles measured on these systems were independent of the degree of cross-linking in the range 0.5−2.0% cross-linker and corresponded to a hexagonal type of structure. Of direct relevance to our results is in particular the fact that the well-ordered structures were no longer found for the longer surfactant hexadecyl sulfate, showing that also here the network constraints suppress self-organization.

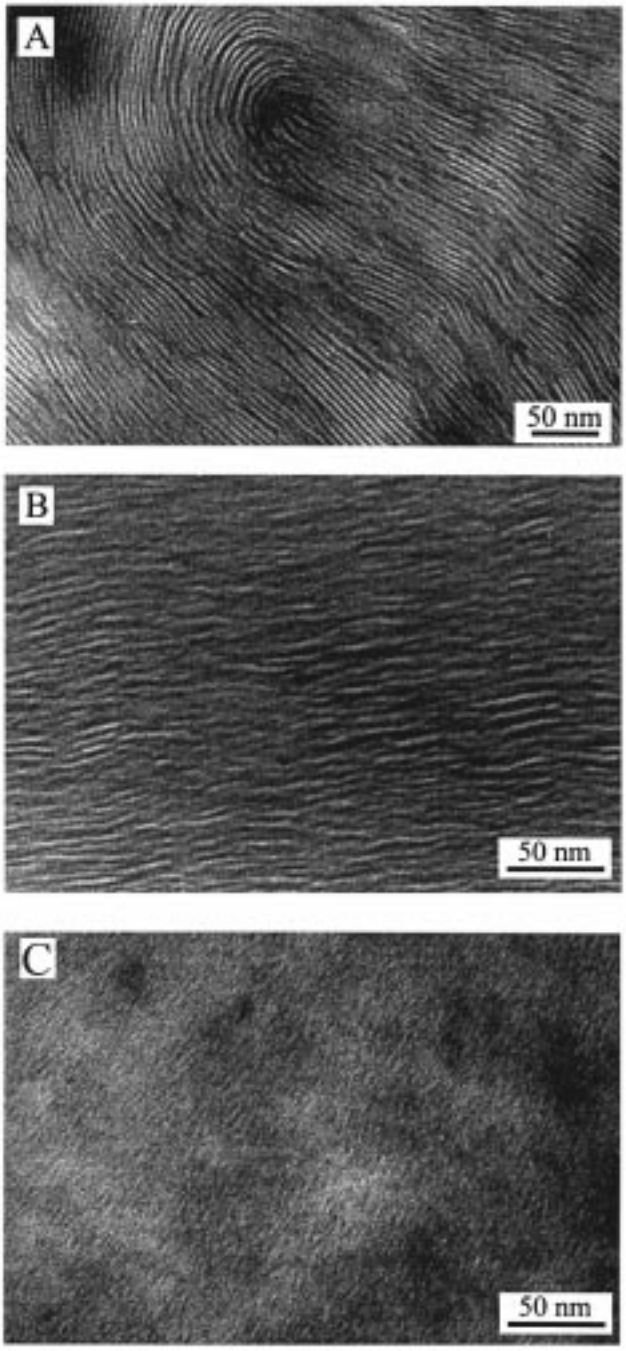

Figure 7. Transmission electron micrographs of (A) P4VP(NDP)$_{1.0}$, (B) P4VP5(NDP)$_{1.0}$, and (C) P4VP20(NDP)$_{1.0}$.

Conclusions

Compared to linear polymers, cross-linked polymer systems offer the distinct advantage of elasticity and orientability. It is therefore satisfying that the concepts developed for nanostructure formation in polymer−amphiphile systems involving hydrogen bonding remain also valid for slightly cross-linked systems. Our results indicate that the network structure does exert an influence on the characteristic parameters of the ordering process, notably on the order−disorder transition temperature and the long period. However, for low degrees of cross-linking this influence is small. On the

other hand, as was to be expected, for sufficiently high degrees of cross-linking ordered structures are strongly suppressed.

Acknowledgment. Dr. A. Hilberer is gratefully acknowledged for preparing the *p*-divinylbenzene, and Juha Tanner is gratefully acknowledged for synthesizing the nonadecylphenol. This work has been supported by the Stichting Scheikundig Onderzoek Nederland (Foundation for Chemistry Research in The Netherlands), the Finnish Academy, Technology Development Centre (Finland), and Neste Foundation. We thank the Institute of Biotechnology of Helsinki University for the use of their electron microscopy facilities.

References and Notes

(1) Kato, T.; Fréchet, J. M. J. *Macromolecules* **1989**, *22*, 3818.
(2) Navarro-Rodrigues, D.; Guillon, D.; Skoulios, A.; Frere, Y.; Gramain, P. *Macromol. Chem.* **1992**, *193*, 3117.
(3) Bazuin, C. G.; Tork, A. *Macromolecules* **1995**, *28*, 8877.
(4) Stewart, D.; Imrie, C. T. *Macromolecules* **1997**, *30*, 877.
(5) Kato, T.; Nakano, M.; Moteki, T.; Uryu, T.; Ujiie, S. *Macromolecules* **1995**, *28*, 8875.
(6) Ruokolainen, J.; Tanner, J.; ten Brinke, G.; Ikkala, O.; Torkkeli, M.; Serimaa, R. *Macromolecules* **1995**, *28*, 7779.
(7) Antonietti, M.; Conrad, J.; Thünemann, A. *Macromolecules* **1994**, *27*, 6007.
(8) Ikkala, O.; Ruokolainen, J.; ten Brinke G.; Torkkeli, M.; Serimaa, R. *Macromolecules* **1995**, *28*, 7088.
(9) Antonietti, M.; Wenzel, A.; Thünemann, A. *Langmuir* **1996**, *12*, 2111.
(10) Antonietti, M.; Burger, C.; Thünemann, A. *Trends Polym. Sci.* **1997**, *5*, 262.
(11) Ober, C.; Wegner, G. *Adv. Mater.* **1997**, *9*, 17.
(12) Tal'roze, R. V.; Platé, N. A. *Polym. Sci.* **1994**, *36*, 1479.
(13) Tal'roze, R. V.; Kuptsov, S. A.; Sycheva, T. I.; Bezborodov, V. S.; Platé, N. A. *Macromolecules* **1995**, *28*, 8689.
(14) Ruokolainen, J.; Torkkeli, M.; Serimaa, R.; Komanschek, B. E.; Ikkala, O.; ten Brinke, G. *Phys. Rev. E* **1996**, *54*, 6646.
(15) Ruokolainen, J.; Torkkeli, M.; Serimaa, R.; Komanschek, B. E.; ten Brinke, G.; Ikkala, O. *Macromolecules* **1997**, *30*, 2002.
(16) Ruokolainen, J.; Tanner, J.; Ikkala, O.; ten Brinke, G.; Thomas, E. L. *Macromolecules* **1998**, *31*, 3532.
(17) Ruokolainen, J.; Mäkinen, R.; Torkkeli, M.; Serimaa, R.; ten Brinke, G.; Ikkala, O. *Science* **1998**, *280*, 557.
(18) Zentel, R. *Angew. Chem. Adv. Mater.* **1989**, *28*, 1407.
(19) Gleim, W.; Finkelmann, H. In McArdle, C. B.; Ed. *Side Chain Liquid Crystal Polymers;* Blackie & Son: Glasgow, 1989.
(20) Wong, G. C. L.; de Jeu, W. H.; Shao, H.; Liang, K. S.; Zentel, R. *Nature* **1997**, *389*, 576.
(21) Okuzaki, H.; Osada, Y. *Macromolecules* **1995**, *28*, 4554.
(22) Dembo, A. T.; Yakunin, A. N.; Zaitsev, V. S.; Mironov, A. V.; Starodoubtsev, S. G.; Khokhlov, A. R.; Chu, B. *J. Polym. Sci., Part B* **1996**, *34*, 2893.
(23) Yeh, F.; Sokolov, E. L.; Khokhlov, A. R.; Chu, B. *J. Am. Chem. Soc.* **1996**, *181*, 6615.
(24) Hilberer, A.; van Hutten, P.; Wildeman, J.; Hadziioannou, G. *Macromol. Chem. Phys.* **1997**, *198*, 2211.
(25) Storey, B. T. *J. Polym. Sci., Part A* **1965**, *3*, 265.
(26) Loshaek, S.; Fox, T. G. *J. Am. Chem. Soc.* **1953**, *75*, 3544.
(27) DiMarzio, E. *J. Res. Natl. Bur. Stand.* **1964**, *A68*, 611.
(28) Ueberreiter, K.; Kanig, G. *J. Chem. Phys.* **1950**, *18*, 399.
(29) Jordan, E. F., Jr. *J. Polym. Sci., Part A* **1971**, *19*, 3367.
(30) De Gennes, P. G. *Scaling Concepts in Polymer Physics;* Cornell University Press: Ithaca, NY, 1979.
(31) Huh, J.; ten Brinke, G.; Ikkala, O. *Macromolecules* **1997**, *30*, 1828.
(32) Hashimoto, T.; Shibayama, M.; Kawai, H. *Macromolecules* **1983**, *16*, 1093.
(33) Mori, K.; Hasegawa, H.; Hashimoto, T. *Polym. J.* (*Jpn.*) **1985**, *17*, 799.
(34) Ehlich, D.; Takenaka, M.; Hashimoto, T. *Macromolecules* **1993**, *26*, 492.

MA9808833